Integration of "omics" strategies for biomarkers discovery and for the elucidation of molecular mechanisms underlying Brugada Syndrome

Domenica Scumaci PhD[#a*], Antonio Oliva MD[#b], Antonio ConcolinoPhD[a], Antonio Curcio MD PhD[c], Claudia Vincenza Fiumara PhD[a], Laura Tammè[a] PhD, Oscar Campuzano BSc, PhD[d,e,f] Vincenzo L. Pascali MD[b], Monica Coll MD PhD[d], Anna Iglesias MD[d], Paola Berne MD[g], Gavino Casu MD[g], Erika Olivo[a], Pietrantonio Ricci MD[f], Ciro Indolfi MD[c] Josep Brugada MD PhD[e,i] , Ramon Brugada MD, PhD[§ d,e,f,j],Giovanni Cuda MD[§a*]

[#]D.S. and A.O. are equally sharing first authorship

[§]R.B. and G.C. are equally sharing senior authorship

[*]Correspondence to:

- Prof Giovanni Cuda, Dpt. of Experimental and Clinical Medicine; Magna Græcia University of Catanzaro,"S.Venuta" University Campus, viale S.Venuta, 88100 Catanzaro phone: +39 0961 3694225, Fax. + 39 0961 3694147, e-mail cuda@unicz.it

- Dr Domenica Scumaci Dpt. of Experimental and Clinical Medicine; Magna Græcia University of Catanzaro,"S.Venuta" University Campus, viale S.Venuta, 88100 Catanzaro phone: +39 0961 3694224, Fax. + 39 0961 3694147, e-mail scumaci@unicz.it

Received: 03 23, 2018; Revised: 05 26, 2018; Accepted: 06 21, 2018

This article has been accepted for publication and undergone full peer review but has not been through the copyediting, typesetting, pagination and proofreading process, which may lead to differences between this version and the Version of Record. Please cite this article as doi: 10.1002/prca.201800065 .

AFFILIATIONS

[a] Department of Experimental and Clinical Medicine; Magna Græcia University of Catanzaro, Catanzaro, Italy.

[b]Institute of Public Health, Legal Medicine Section, Catholic University, School of Medicine, Largo Francesco Vito 1, 00168, Rome, Italy.

[c] Division of Cardiology, Department of Medical and Surgical Science, University "Magna Graecia" of Catanzaro, Italy

[d] Cardiovascular Genetics Center, Gencardio Institut d'Investigacions Biomèdiques de Girona (IDIBGI) Girona- Spain

[e] Centro de Investigación Biomédica en Red de Enfermedades Cardiovasculares (CIBERCV), Spain

[f] Department of Medical Sciences, School of Medicine, University of Girona, Girona, Spain

[g] Unità Operativa Complessa di Cardiologia Ospedale “San Francesco”, Nuoro, Italy.

[h] Institute of Legal Medicine, University "Magna Graecia" of Catanzaro, Italy.

[i] Arrhythmia’s Unit, Hospital Clinic, Barcelona, Spain.

[j] Cardiology Service, Hospital Josep Trueta, Girona, Spain

STATEMENT OF CLINICAL RELEVANCE

BrS is a life threatening cardiac disorder, whose molecular basis has not been fully defined yet–due to the genetic/phenotypic heterogeneity. Data presented in this paper, even though referred to a small group of patients, provide interesting and original insights into novel circulating biomarkers in BrS, which might be helpful for boosting the development of new strategies for diagnosis.

ABSTRACT

Purpose

The Brugada syndrome (BrS) is a severe inherited cardiac disorder. Given the high genetic and phenotypic heterogeneity of this disease, we integrated in a synergic way three different "omics" approaches to elucidate the molecular mechanisms underlying the pathophysiology of BrS, as well as for identifying reliable diagnostic/prognostic markers.

Experimental design

We performed the profiling of plasma Proteome and MiRNome in a cohort of Brugada patients that were preliminary subjected to genomic analysis to assess a peculiar gene mutation profile.

Results

The integrated analysis of "omics" data unveiled a cooperative activity of mutated genes, deregulated miRNAs and proteins in orchestrating transcriptional and post-translational events that are critical determining factors for the development of the Brugada pattern.

Conclusions and clinical relevance

Our study provides the basis to shed light on the specific molecular fingerprints underlying BrS development and to gain further insights on the pathogenesis of this life-threatening cardiac disease.

KEY WORDS

Brugada syndrome; Genomics; Proteomics; MiRNA; MAPK; ROS

Abbreviation

MAPK, mitogen-activated protein kinase; ROS, Reactive oxygen species; BrS, Brugada syndrome; ECG, electrocardiogram; SD, sudden death; 2DE, two-dimensional gel electrophoresis; LC-MS/MS Liquid chromatography tandem-mass spectrometry; NGS, next generation sequencing; RT-qPCR, reverse transcription real-time polymerase chain reaction.

INTRODUCTION

The Brugada syndrome (BrS) is an inherited cardiac disorder responsible for 5-12% of sudden death (SD) in otherwise healthy individuals, representing one of the most common causes of cardiac death among young adults, especially men nearly 40 years of age. [1] Main characteristics of BrS are ST-segment elevation in the right precordial leads of the electrocardiogram (so-called type 1 ECG) and ventricular tachyarrhythmias that predispose patients with structurally normal hearts to-SD. Therefore, an early identification as well as an accurate risk stratification are crucial in order to avoid lethal episodes. The first gene to be linked to BrS was SCN5A, encoding for the sodium voltage-gated channel α-subunit 5. Currently, in patients with BrS more than 300 pathogenic variants in more than 16 genes have been detected, which can be classified in four main sub-categories: i) loss of function of sodium channels; ii) loss of function of calcium channels; iii) gain of function of potassium channels; iv) alterations of other regulatory proteins. [2] Despite important advances in last years, current diagnostic strategies need to be improved.

Given the high genetic and phenotypic heterogeneity of this disease, it has become increasingly clear that integrated approaches are needed in order to shed light on the complexity of the molecular mechanisms underlying the pathophysiology of BrS, as well as on the identification of reliable diagnostic/prognostic markers.

Circulating biomarkers, such as proteins and micro-RNAs (miRNAs), can be highly informative, mainly because of their activation either before the clinical onset of the disease, or after the presence of an overt disease status.

In this regard, proteomics is a valuable tool for biomarker discovery since it favors the comparison among hundreds of proteins in several samples in a single experiment.

In recent years, the focus has moved to plasma biomarkers, considering that each cell in the organism produces a number of normal or abnormal products, which eventually reach the bloodstream as a waste or as signaling molecules. [3,4]

Although the dynamic range of plasma proteins spans over 10 orders of magnitude with the consequence that potential biomarkers could be entirely masked by the overwhelming abundance of few proteins, [5] the combination of Protein equalizer technology (Proteominer)[6,7] with two-dimensional gel electrophoresis (2DE), and mass spectrometry (MS), allows the simultaneous assay of hundreds of proteins in a given sample. This approach bypasses the depletion of high abundant proteins that may cause the loss of potentially critical information. [5]

Using this strategy, our group has previously identified potential plasma biomarkers in a family with BrS sharing a heterozygous nonsense variant in the *SCN5A* gene. [8]

Additionally, a class of genetic, epigenetic and translational regulators called miRNAs, are currently considered plasma circulating biomarkers as well.

Besides regulation of basic biological processes including development, differentiation, apoptosis, fibrosis and proliferation, miRNAs finely tune numerous properties of cardiac excitability including conduction, repolarization, automaticity, Ca^{2+} handling, and spatial heterogeneity of impulse propagation. [9-13]

In the current literature, a large number of studies are based on the use of individual classes of biomarkers. In our opinion, however, a synergistic analysis of different categories of potentially interesting biomolecules, each reporting information on distinct mechanisms involved in a specific disorder, might turn up to be more informative and useful.

For the present study, we selected a cohort of BrS patients that were preliminary subjected to genomic analysis to identify the genetic variants involved in the pathogenesis of the syndrome. In addition, an integrated study of the proteome and miRNome was performed to

uncover novel diagnostic/prognostic markers and to shed further light on the molecular mechanisms underlying this complex and intriguing cardiac disorder.

MATERIAL AND METHODS

Patients enrollment

The study was approved by the "Comitato Etico Azienda Ospedaliera Universitaria Mater Domini" University Magna Graecia of Catanzaro. Blood samples were obtained from each affected patient and family members after signing informed consent. Fifteen subjects were enrolled in the study.

All enrolled patients were asymptomatic and presented a diagnostic ECG pattern for Brugada syndrome (type 1 ECG Brugada pattern), characterized by J-point elevation ≥2 mm in one or more leads among the right precordial leads V1 and/or V2 positioned in the fourth, third, or second intercostal space, followed by a coved-type ST-segment and a negative T wave, either spontaneously or after intravenous administration of ajmaline (1 mg/Kg over 10 minutes). All patients underwent echocardiography to rule out underlying structural cardiac disease. Five patients were probands, and the remaining 10 were diagnosed during family screening for BrS.

Patients enrollment for test set.

Samples were collected at the Cardiology Unit, Magna Graecia University, Medical School, Catanzaro, Italy, and officially registered. All patients and healthy relatives were asked to give informed written consent approved by the ethical committee of the Medical School. Diagnosis of BS was made by two distinct physicians according to clinical and instrumental manifestations; the presence of a heterozygous nonsense variant (Q1118X) in the *SCN5A* gene was demonstrated in the proband and in 6 relatives by genetic analysis. [8]

GENETICS SECTION

DNA samples

First, genomic DNA from 15 BrS patients was extracted with Chemagic MSM I from peripheral blood (Chemagic human blood- Chemagen) and the concentration was checked by fluorometry (Qubit, Life Technologies). Purity was measured with NanoDrop1000 spectrophotometer (Thermo scientific) to assess quality ratios of absorbance. DNA integrity was assessed on a 0.8% agarose gel. DNA sample was fragmented by Bioruptor (Diagenode). Library preparation was performed according to the manufacturer's instructions (SureSelect XT Custom 0.5–2.9 Mb library, Agilent Technologies, Inc). After capture, the indexed library was sequenced in a six-sample pool cartridge. Sequencing process was developed on MiSeq System (Illumina) using 26150 bp reads length.

Custom resequencing panel

A custom resequencing panel including 55 genes was applied (table 1). This panel includes the most prevalent genes involved in SD-related pathologies, according to available scientific literature. The genomic coordinates corresponding to these 55 genes were designed using the tool eArray (Agilent Technologies, Inc.). All the isoforms described at the UCSC browser were included at the design. The final size was 432,512 kbp of encoding regions and UTR boundaries. The coordinates of the sequence data is based on NCBI build 37(UCSC hg19).

Bioinformatics analysis

Mapping DNA reads to an annotated reference sequence and determining the extent of variation from the reference. An in-house pipeline for secondary data analysis was developed.

To increase the quality of the analysis, reads from FASTQ files were trimmed based on the quality of the last nucleotides towards the 5' ends. The processed reads were mapped with GEM Mapper.[14] The output from mapping steps was joined and sorted. Only the uniquely and properly mapped read pairs were selected. Finally, the cleaned BAM file was annotated with SAM tools v.1.18 [15], GATK v2.4,[16] together with an *ad hoc* developed method to generate the first raw VCF files. Variants were annotated with dbSNP IDs, Exome Variant Server (EVS) [17] and the 1000 Genomes browser. [18]

Tertiary analysis was then performed. For each genetic variant identified, allelic frequency was consulted in ExAC, EVS, and 1000 genomes databases. In addition, HGMD [19] was also consulted to identify pathogenic mutations previously reported. Regarding novel genetic variants, *in silico* prediction of pathogenicity was assessed using PROVEAN,[20] PolyPhen-2,[21] and Mutation Assessor.[22]

Genetic confirmation

To confirm the results obtained after NGS, conventional Sanger sequencing was applied to the genomic DNA. Polymerase chain reaction (PCR) was used to amplify the exons where the rare genetic variants were found by NGS. The PCR product was purified by ExoSAP-IT (USB Corporation, Cleveland, OH, USA) and directly sequenced by dideoxy chain-termination method in ABI Prism Big Dye® Terminator v3.1 Cycle Sequencing Kit (Applied Biosystems, USA). Sequencing was processed in a 3130XL Genetic Analyzer (Applied Biosystems) and analyzed by means of the SeqScape Software v2.5 (Life Technologies) comparing the obtained results with the reference sequence from hg19. Protein numbering reflects the translation initiator Methionine numbers as +1.

PROTEOME PROFILING

Sample collection

Plasma samples were obtained according with Plasma Proteome Project guidelines; we collected 15 plasma samples from patients with inherited BrS (Table 2) and 15 plasma samples from healthy volunteers, based on clinical observations. Cases and controls were age and sex matched. Approximately 4 ml of blood were drawn by venipuncture and collected in K_2EDTA tubes. The samples were centrifuged within 2 hours of collection at 1,300 x g for 10 minutes, and resulting plasma was aliquoted into silicone tubes and stored at -80°C until use.

Sample preparation for ProteoMiner

Plasma samples were treated with combinatorial peptide ligand library (CPLL) provided by the ProteoMiner kit according to the manufacturer's protocol. [7]

This technology is based on the treatment of complex biological specimens with a large hexapeptide library bound to a chromatographic support. Each hexapeptide is able to bind to a unique protein and the binding is limited by the bead capacity. Under these conditions, high-abundance proteins rapidly saturate their ligands; on the other hand, low-abundance proteins are concentrated on their specific hexapeptides, thereby decreasing the dynamic range of proteins in the sample.

Briefly, the column was washed three times with PBS buffer. Subsequently, 1 ml of diluted human plasma pool containing 60 mg of proteins was added to the column and incubated at room temperature for 2 h with gentle shaking. The proteins bound to the beads containing combinatorial peptide ligands were washed three times and eluted with 100 µl of elution buffer for three times, accordingly with manufacturer's instructions. Proteins, eluted in three sequential steps, were pooled together and stored for future experiments.

1-D SDS PAGE

Following ProteoMiner enrichment, total protein content of plasma samples was determined using the Bradford Protein Assay (Bio-Rad) according to the manufacturer's instructions with human serum albumin (Sigma Aldrich) as standards. [23]

Samples of crude and treated plasma were analyzed by one dimensional sodium dodecyl sulphate polyacrylamide gel electrophoresis (1D-SDS-PAGE) to assess quantitative/qualitative differences in protein profiles. Briefly, for SDS-PAGE, 20 µg of each sample were diluted with Laemmli buffer, incubated at 100 °C for 5 min, and loaded onto a 12% SDS-polyacrylamide gel. Separation was achieved at 80 V.[24] Resulting Gel was stained with EZBlue™ Gel Staining Reagent, (Sigma Aldrich).

2D Gel electrophoresis analysis

After ProteoMiner treatment, plasma samples were pooled to create three groups (*SCN5A* variant positive BrS patients, *SCN5A* variant negative BrS patients and controls subjects) with the aim to minimizing intra-class sample variability. Resulting pools were subjected to high-resolution 2DE. [25-27]. For each pool, 130 µg of proteins were diluted into Isoelectrofocusing (IEF) sample buffer containing 8 M urea, 4% CHAPS, 0.1 M DTT, 0.8% pH 3–10 nonlinear (NL) carrier ampholyte buffer. IEF was carried out on non-linear immobilized pH gradients (pH 3–10 NL; 24-cm-long IPG strips; GE Healthcare). The first dimension was run on a GE Healthcare IPGphor unit, and a total of 70 000 Vh was applied. Prior to SDS-PAGE, IPG strips were equilibrated with a dithiothreitol (10 mg/mL) SDS equilibration solution followed by a treatment with iodoacetamide (25 mg/mL) SDS equilibration solution as described in the GE Healthcare Ettan DIGE protocol. Second dimension separation was carried out on 10% SDS-polyacrylamide gels, (2W/gel; 25°C) until the bromophenol blue dye front reached the end of the gels. [28] MS-compatible silver

staining protocols was used to stain resulting gels.[29-30] Each pooled analysis was performed in triplicate.

The software Image master 2D-Platinum, version 6.0 (GE Healthcare), was used to perform gel image analysis. The spot auto-detect function was applied for all group comparisons using identical parameters. Groups were matched automatically and corrected manually if necessary. Differences in protein expression were identified using the relative volume (%Vol). Applying this option, data became independent of experimental variations caused by differences in loading or staining.[31] Analysis was performed using three independent experiments, respectively. All data were presented as mean ± SEM (N=3), where SEM represents the standard error of the mean and N specifies the number of experimental biological replicates.

Protein levels in each data set were compared to control group using unpaired t-test. A two-sided p-value < 0.05 was considered statistically significant. Data were plotted using Excel spreadsheet (Microsoft).

Electrophoretic spots, obtained from analytic 2D gels, were manually excised, destained, and acetonitrile-dehydrated. The eluted proteins were then digested using an in-gel procedure as previously described. [32]

The resulting tryptic peptides were purified by Pierce C18 Spin Columns (Thermo Fisher Scientific Inc.) according to the manufacturer's procedure, eluted with 40µL of 70% acetonitrile and dehydrated in a vacuum evaporator.[33] Each purified tryptic peptide was finally analyzed through Nanoscale LC-MS/MS.

Nanoscale LC-MS/MS analysis

LC-MS/MS analysis was performed using an Easy LC 1000 nanoscale liquid chromatography (nanoLC) system (Thermo Fisher Scientific, Odense, Denmark). The

analytical nanoLC column was a pulled fused silica capillary, 75 μmi.d., in-house packed to a length of 10 cm with 3 μm C18 silica particles from Dr. Maisch (Entringen, Germany). The peptide mixtures were loaded at 500 nL/min directly onto the analytical column. A binary gradient was used for peptide elution. Mobile phase A was 0.1% formic acid, 2% acetonitrile, whereas mobile phase B was 0.1% formic acid, 80% acetonitrile. Gradient elution was achieved at 350 nL/min flow rate, and ramped from 0% B to 30% B in 15 minutes, and from 30% B to 100% B in additional 5 minutes; after 5 minutes at 100% B, the column was re-equilibrated at 0% B for 10 minutes before the following injection. MS detection was performed on a quadrupole-orbitrap mass spectrometer Q-Exactive (Thermo Fisher Scientific, Bremen, Germany) operating in positive ion mode, with nanoelectrospray (nESI) potential at 1800 V applied on the column front-end via a tee piece. Data-dependent acquisition was performed by using a top-5 method with resolution (FWHM), AGC target and maximum injection time (ms) for full MS and MS/MS of, respectively, 70,000/17,500, 1e6/5e5, 50/400. Mass window for precursor ion isolation was 2.0 m/z, whereas normalized collision energy was 30. Ion threshold for triggering MS/MS events was 2e4. Dynamic exclusion was 15 s.

Data were processed using Proteome Discoverer 1.3 (Thermo Fisher Scientific, Bremen, Germany), using Sequest as search engine, and the HUMAN-refprot-isoforms.fasta as sequence database. The following search parameters were used: MS tolerance 15 ppm; MS/MS tolerance 0.02 Da; fixed modifications: carbamidomethylation of cysteine; variable modification: oxidation of methionine, phosphorylation of serine, threonine and tyrosine; enzyme trypsin; max. missed cleavages 2; taxonomy Human.

Protein hits based on two successful peptide identifications (Xcorr> 2.0 for doubly charged peptides, >2.5 for triply charged peptides, and >3.0 for peptides having a charge state >3) were considered valid.

Western blotting analysis

Equal amounts of total proteins (50μg) from each specimen were used to perform quantitative western blotting analysis and to validate a subset of candidate biomarkers. Proteins of crude plasma samples were resolved on 12% SDS-polyacrylamide gel, electrophoresed at 100 V for 2 h, and blotted onto nitrocellulose membranes by electrotransfer using Turboblot (Biorad). The electrophoretic bands were blocked with 5% nonfat dry milk/PBS (MPBS), 0.2% Tween 20 for 1 h at room temperature, after controlling the amount of total protein loaded on each lane by the Ponceau red staining (Sigma-Aldrich),each membrane was incubated with the specific antibodies at the following dilutions: Mouse monoclonal (B9) to alpha1 Antitrypsin (Abcam) 1:500; Mouse monoclonal ApoE (D6E10) sc-58242 (SantaCruzBiotecnology) 1:1000; Vitronectin Rabbit monoclonal Antibody (Epitomics) 1:1000.

The signal was detected using anti-mouse horseradish peroxidase-conjugate secondary antibodies (Cell Signaling) for mouse primary antibody, antirabbit horseradish peroxidase-conjugate secondary antibodies (Cell Signaling) for Rabbit primary antibody and ECL reagent (Santa Cruz Biotechnology). HRP-conjugated γ-Tubulin (clone C-20, Santa Cruz) was used at a final concentration of 1μg/ml to ensure equal amount of protein loading. Blots were developed using the SuperSignal West Femto ECL substrate (Pierce, EuroClone). Densitometric software (Alliance 2.7 1D fully automated software) determined the percent distribution of blotted proteins after image acquisition by Alliance 2.7 (UVITEC, Eppendorf, Milan, Italy).

Data were analyzed and plotted using Excel spreadsheet (Microsoft), and expressed as mean±SEM (N), where SEM represents the standard error of the mean and N indicates the number of experimental repeats. Unpaired t-test was used to compare protein levels in each data set. A two sided p-value <0.05 was considered statistically significant.

To normalize the protein loading for the plasma samples during Western blot analysis, as there are no housekeeping genes, the Ponceau red stained membranes were densitometrically scanned and images were analyzed using Alliance 2.7 1D fully automated software. The values obtained were then used to cross normalize the densities of bands corresponding to analyzed proteins.

MiRNA PROFILING

miRNA panel

For miRNAs profiling, total RNA was extracted from plasma using the miRCURY™ RNA Isolation Kit - Biofluids (Exiqon, Denmark) according to the manufacturer's instructions. Briefly, plasma was thawed on ice and centrifuged at 3,000xg for 5 min in a 4 °C microcentrifuge. An aliquot of 200 µL of plasma per sample was transferred to a new microcentrifuge tube and 60 µL of Lysis solution was added. The tube was mixed and incubated for 3 min at room temperature. Twenty µL of Protein Precipitation Solution was added to the mixture, incubated for 1 min at room temperature and centrifuged for 3 min at 11,000xg. The supernatant was transferred to a new microcentrifuge tube and 270 µL of isopropanol was added. The contents were mixed thoroughly and transferred to a Qiagen RNeasy® Mini spin column in a collection tube followed by centrifugation at 11,000 x g for 30 sec at room temperature. The process was repeated until all the remaining samples had been loaded. Total RNA was eluted by adding 50 µL of RNase-free water to the membrane of the Qiagen RNeasy® mini spin column and incubating for 1 min before centrifugation at 11,000 x g for 1 min at room temperature. The RNA was stored in a − 80 °C freezer. RNA concentration and purity were evaluated using Nanodrop (Thermo Scientific). miRNAs were reverse-transcribed using the miRCURY LNA™ Universal RT miRNA PCR,

Polyadenylation and cDNA synthesis kit (Exiqon, Denmark). cDNA was diluted and assayed in PCR reactions according to the protocol for miRCURY LNA™ Universal RT miR PCR. For the screening, each miRNA was assayed in triplicate by qPCR on the miRNA Ready-to-Use PCR plates. Each panel contains LNA™ primers for 179 human serum/plasma microRNAs, control and reference assays. DNA and RNA spike-ins were included in the qPCR and RT step, to supervise extraction and amplification steps. Negative controls excluding template from the reverse transcription reaction were conducted and profiled like the samples. The amplification was performed in the iQ5 real-time PCR detection system (Bio-rad) in 96 well plates using cycling parameters recommended by Exiqon. The amplification curves were analyzed using the iQ5 Optical System Software, both for determination of crossing points (Cp) and for the melting curve analysis. The median of triplicate probes was used for each array, and expressed data were normalized using the median normalization method.

Data analysis was performed using GenEx2.0 Software. Data was managed according with software instruction. We compared the miRNA profile of BrS patients either positive and negative for *SCN5A* variant with control group. Analyses were done using unpaired Student's test. All tests were done two-tailed and P value was adjusted for multiple comparisons using Bonferroni correction and set at <0.035 for significance.

Candidate miRNA confirmation and quantification by Taqman real-time quantitative PCR

TaqMan MicroRNA assay (Life Technologies, Inc.) was used for specific miRNA assays. Ten ng of total RNA of plasma was used to perform RT using miRNA specific primers for three candidates (miR-425-5p, miR-320b and miR-92a-3p) and for endogenous control (miR-93-5p) as per manufacturer's protocol (Life Technologies Inc.).

Reverse transcription (RT) was performed with TaqMan miRNA RT Kit (Life Technologies, Carlsbad, CA, USA) according to manufacturer's protocols. RNA concentration and purity

were evaluated using Nanodrop (Thermo Scientific) and used as template RNA (10 ng serum miRNA) for RT reactions.

Briefly, RT reaction mixture contained 3 µL of 5X RT primer, 0.15 µl 100 mM dNTPs (with dTTP), 1 µl multiscribe reverse transcriptase (50 U/µ l), 1.50 µ l 10X RT Buffer, 0.19 µlRNAse inhibitor (20 U/µ l), RNA template and nuclease-free water to a final volume of 15 µl. RT reaction was carried out on Veriti 96-Well Thermal Cycler (Life Technologies, Carlsbad, CA, USA) according to manufacturer's recommended thermal cycling conditions. Reactions were held on ice for at least 5 min, followed by incubation in a thermal cycler at 16°C for 30 min, 42°C for 30 min, 85°C for 5 min, and hold at 4°C.

miR-93-5p, which gave the most stabilized expression both in control and Brugada syndrome samples, was used as an endogenous control for the validation of all selected candidate miRNAs.

Real-time qPCR was performed using a TaqMan MicroRNA assay to quantitate individual miRNAs. Briefly, 1.33 µl of RT product was used along with 10 µl of TaqMan preamp mastermix along with 1µl 0.2X TaqMan small RNA assay (20x) and nuclease free water to a final volume of 20 µl. The thermal cycling conditions for the iQ5 instrument consist of an initial denaturation at 95°C for 10min, and 45 cycles of 95°C for 15 sec, 60°C for 60 sec.

TaqMan miRNA assays were carried out in triplicates to validate the changes in level of expression for some Brugada syndrome candidate miRNAs. Each miRNA was calibrated to a selected endogenous control miR-93-5p to get a delta Ct (ΔCt) value for each miRNA (miRNA Ct value– miR-93-5p Ct value). The fold changes were then calculated using the comparative Ct method ($2^{-\Delta\Delta Ct}$).

The amplification curves were analyzed using the iQ5 Optical System Software, both for determination of crossing points (Cp) and for the melting curve analysis. The median of

triplicate probes was used for each array, and expressed data were normalized using the median normalization method.

BIOINFORMATIC ANALYSIS

Pathway analysis

Ingenuity Pathway analysis (Ingenuity Systems, www.ingenuity.com) was performed to examine functional correlations within differentially expressed proteins and miRNAs. IPA constructs hypothetical protein interaction clusters based on a regularly updated Ingenuity Pathways Knowledge Base.

Data sets containing proteins and miRNAs identifiers and corresponding expression values were uploaded into the application. Molecules differentially expressed, with a fold change of at least ±1.5, were overlaid onto global molecular networks developed from information contained in the knowledge base. Networks were then algorithmically generated based on their connectivity. Networks were "named" on the most common functional group(s) present. Canonical pathway analysis acknowledged function-specific proteins significantly present within the networks.[34] Each analysis was statistically evaluated by the Fischer exact test. This was used to calculate a p-value determining the probability that each biological function and/or disease assigned to that network is due to a random event.

RESULTS

A total of 27 rare genetic variants were identified in 14 cases (Table 2). Only in one case (index case 15) no mutations were found. At least one variant was identified in each case analyzed. New genetic variants in the *SCN5A*, *TTN*, *ANK2*, and *VCL* genes were detected in 5 cases showing showing restricted segregation after screening the family members.. Other rare

genetic variants were detected in 8 cases but without available DNA of relatives in order to perform familial segregation: *TTN, SGCA, CACNA1D, JUP, SCN5A, DSC2, JPH2, DSP, TCAP* genes. Lack of segregation was observed after familial screening only in 1 case (Table 2).

Segregation studies

Segregation studies were performed in 5 available families.. The analysis showed restricted segregation due to lack of parent's sample (Index cases 1-5, Figure 1): p.V1415M_*SCN5A* (Figure 1A); p.K21298N_*TTN* (Figure 1B); p.D1802E_*SCN5A* and p.K14782R_*TTN* (Figure 1C); p.T1612A_*ANK2* and p.Q1017H_*VCL* (Figure 1D); and p.E1061X_*SCN5A* (Figure 1E). One of the studied families did not show segregation (Index case 14): p.R1194Q_*CACNA1H* and p.P307S_*KCNA5* (Supplementary Figure 1).

1D gel analysis before and after ProteoMiner enrichment

Plasma samples of control subjects and BrS patients were incubated with ProteoMiner beads to reduce the dynamic range of protein concentration, and subsequently analyzed by 1D SDS PAGE. As presented in Supplementary Figure 2, comparing the proteins profile of non-fractionated plasma (lanes 2 and 4) with that of ProteoMiner-treated plasma (lanes 3 and 5), there was a significant reduction in the amount of most abundant proteins (e.g. albumin and IgG light/heavy chains), and a concomitant enrichment in less abundant proteins, as suggested by the appearance of new protein bands in the low molecular weight region (below 35kDa).

2DE analysis

ProteoMiner eluates from BrS patients positive for *SCN5A* variants, BrS patients negative for *SCN5A* variants and control subjects were analyzed by 2DE gels. Figure 2A shows representative 2D maps. Gel maps were analyzed using Image master 2D platinum. After automatic spot detection, background subtraction and volume normalization, 1097±45 spots were detected in control sample maps, while 1101±38 were detected in BrS samples (*SCN5A* positve) and 1106±32 in BrS samples (*SCN5A* negative). Only reproducibly detected spots were subjected to statistical analysis. Following the comparative analysis, 68 spots resulted significantly deregulated in BrS samples versus controls. The comparative analysis allows us to conclude that patients positive for *SCN5A* variants as well as patients negative for *SCN5A* have a very similar omics pattern profile.

Among the differentially expressed proteins, 30 were up-regulated while 38 were down-regulated. Following the comparative analysis, the 68 spots of interest were manually excised from the gels, trypsin-digested, and subjected to LC-MS/MS analysis. A list of up- or down-expressed proteins and the relative identifications is provided as Supplementary Table 1.

Western blot validation

Western blot analysis was performed on three differentially expressed proteins to confirm 2DE gels results. The analysis was done on unfractionated plasma samples to exclude artifacts due to the enrichment system. The selection of proteins to be confirmed by western blot was based on our previously published proteomic data and current literature.[8] As expected, blot analysis confirmed that Apoliprotein E and Vitronectin were significantly upregulated in the plasma samples of BrS subjects versus controls whereas α-1-antitrypsin was downregulated (Figure 2B).

MiRNA profiling

MiRNA profiling was done using Serum/Plasma Focus microRNA PCR Panels I and II (ExiqonInc.). The qPCR devices contained inter-plate as well as reverse transcription calibrators. These were used to normalize the data after it was exported to Genex software v.6.1 (ExiqonInc).

In plasma samples there is always a risk that hemolysis has occurred while handling the blood samples, giving rise to cellular derived microRNA contamination. The plates included a way of testing for hemolysis that consisted in monitoring the ΔCt between has-miR-23a-3p and has-miR-451a. The quality control test, performed with Genex, assessed that all the plasma samples included in the study have a ΔCt less than 7, accordingly with the criteria of inclusion provided by device's manufacturer.

Moreover, the Genex function NormFinder was used to find the miRNA detected in all samples to be the best normalizer. All the data was normalized according to miRNAs 93-5p as reference.

Normalized values for all BrS patients vs. controls were subjected to a fold-change analysis. Statistical analysis was performed using Student t-test. *P* value was adjusted for multiple comparisons using Bonferroni correction and set at <0.037 for significance.

To investigate a possible difference in miRNA expression profile between BrS patients and healthy subjects, 179 miRNAs were assessed in plasma from 13 patients with Brugada syndrome and 10 healthy blood donors. Patients with BrS were clustered in two groups, subjects that carry a variant on SCN5A gene and subjects negative for SCN5A variant that carry a mutations on a gene candidate to be associated with Brugada syndrome. Patient's characteristics are summarized in Table 2. BrS patients, either negative and positive for SCN5A variants, show a similar trend in the miRNAs expression pattern compared to controls.A total of 28 miRNAs were differentially expressed *(Bonferroni p<0.035),* of which 17 were downregulated and 11 were upregulated (Figure 3, panel a).

To confirm the Brugada miRNA profiling, Taqman qPCR assays were performed; the analysis was done on three miRNAs, i.e. miR-92a, miR-320b and miR-425-5p, whose expression is related with cardiovascular diseases. MiR 93-5p was used as reference miRNA for comparative Ct method.

Taqman assay confirmed that miR-425-5p was considerably decreased, while miR-320b and miR-92a-3p were significantly increased in Brugada syndrome plasma samples (either positive and negative for *SCN5A* variants) vs. control subjects~~,~~ (Figure 3, panel b, c, d).

Ingenuity Pathway Analysis

Proteins and miRNAs differentially expressed in BrS patients vs. ~~healthy~~ controls were connected predominantly to canonical pathways as LXR/RXR Activation, Acute Phase Response Signaling, FXR/RXR activation, and Coagulation System (Supplementary Figure 3).

Deregulated molecules were mapped into six main networks of interacting protein clusters (Figure 4a). The most representative were the first two (Figure 4b, and c), with scores of 28 and 15 focus molecules, each. The largely represented molecules were those associated with vascular diseases, including angiogenesis, vasculogenesis, thrombus formation, acute coronary syndromes and peripheral vascular disease.

IPA also depicted cardiovascular diseases associated with the networks of interest (categories listed in Supplementary Table 2).

Finally, in order to condense the IPA-identified networks, MAP (Molecule Activity Predictor), a function that anticipates the upstream/downstream effects of activation or inhibition of molecules included in the analyzed dataset, established the *in-silico* up regulation of Erk1/2 pathway (Supplementary Figure 4). Remarkably, by investigating the relationships between deregulated molecules and mutated genes that showed segregation in

BrS, it was possible to map 173 pathways overlapping the dataset of deregulated proteins and miRNAs, which depicted ERK1/2 as focal hub. (Supplementary Figure 5).

Implication of genetic variations in omics dataset.

Using IPA tool we investigated the most interesting connection between mutated genes and omics dataset. As previously reported, we mapped 173 pathways linking affected genes and deregulated omics dataset. Here are details the most intriguingly relations.

In our opinion, it is singular that *SCN5A, TNT, VCL* and *ANK2* are all able to affect the activity of TP53, the first directly, and the others through the interaction with Cdk2.[35-38-77] TP53 is a key regulator of miRNA biogenesis.[39] In our model, IPA analysis predicts also the down regulation of TP53. The reduction of the levels of TP53 should be determinant for the induction of miR320,[40] whose high levels are reported to be related with an increased risk of infarction.[41]

It is also described that the one by one interference of *SCN5A, ANK2 or VLC* gene, produces the activation of MAPK pathway.[42-44]

The activation of this pathway might be crucial for the up regulation of Complement C3.[43]

Interestingly, several proteins dysregulated in the blood of patients either carrying or not a peculiar genetic variation on *SCN5A gene* compared to control subject, seem to have a key role in cardiovascular pathophysiology. We assessed the upregulation of Complement C3 concomitantly with a down regulation of FGB coherently with the finding that high levels of C3 protein as well as low levels of FGB increase size of infarct.[45, 46]

TNT mutations are reported to negatively affect the expression of miR425.[47] Low levels of mir425 induce the over expression of IL24,[48] a well-characterized cytokine increasing the production of ROS.[49] The down regulation of miR425, through IL24 upregulation, might

account for the decrement of vimentin, [50-51] and for the up-regulation of Alpha-2-macroglobulin and Apolipoprotein A4. [52-54]

VNC is able to affect the expression of interleukin 6 whose up regulation might be determinant for the up regulation of Fibrinogen gamma chain, alpha-2-macroglobulin, complement C3 and miR 342-3p. [56-59]

pErk 1/2 expression validation

The upregulation of pErk1/2 was confirmed using western blot analysis on BrS plasma and control samples. PhosphoErk1/2 signal was normalized using the total Erk1/2. As shown in figure 4d, pErk was indeed clearly up-regulated in the plasma of BrS patients compared to control subjects.

The upregulation of pErk1/2 was further confirmed in a test set of brugada patients. (Figure 4e)

In silico ROS activation prediction

Since IPA revealed increased production of reactive oxygen species (ROS) as well (Supplementary Figure 3), we further investigated the link between deregulated proteins/miRNAs and ROS pathways. The software defined 1315 pathways connecting the members of the "-omics" data set with ROS generation. Using our quantitative data and the IPA MAP function, it was possible to predict a peculiar overexpression of ROS (Supplementary Figure 6).

DISCUSSION

In this study, we show the results of an integrated genetic, proteomic and miRNomic analysis conducted on plasma samples from individuals with BrS. To this aim, we have enrolled 15 BrS patients, belonging to five families in which segregation analysis demonstrated a potential positive score for the following genes: *SCN5A, VCL, TTN* and *ANK2*. Only one subject (index case 15) did not show any genetic variants.

The number of patients enrolled for the study is justified by the low prelevance of the syndrome wandering around 0.01%-0.3% in function of regions and ethnicities. [60]The *SCN5A* gene is the most frequently affected by pathogenic variants in BrS patients [2,61,62]. Our data show that in spite of 33% *SCN5A* alterations, the identification of genetic variants in remaining 9 cases should be cautiously considered, since our multilevel examinations provide sufficient evidences that different genes, and various mutations, share common focal hub associated with BrS appearance. To this regard, two patients in our group (#4 and #10) presented a SCN5A variant, p.L1501V, which has been associated, as other genetic alterations, with only minor biophysical defects of the sodium channel itself [63]. However the finding of concurrent variants in these BrS patients affecting vinculin (VCL), and ankyrin (ANK2) genes, which have not been directly linked to BrS so far [2,61], focuses the attention on the final common pathways that we observed in our "–omics" integrated approach. In fact, vinculin protein plays a structural role in ventricular myocytes that, when disrupted, can lead to contractile dysfunction and dilated cardiomyopathy (DCM) [64].

Ankyrin protein is required for membrane targeting and stability of Na^{+}/Ca^{++} exchanger in cardiomyocytes, and loss of its interaction with the sodium channel has been related to cardiac arrhythmias [65].

The translated product of the *TTN* gene is Titin protein. This high molecular weight protein provides connections at the level of individual microfilaments and it contributes to the fine balance of forces between the two halves of the sarcomere. Genetic variations in the *TTN*

gene have been associated with DCM; however, studies in different cohorts of patients identified variants of unknown significance in this gene. [66]

In cardiovascular medicine, the translation of proteomic discoveries has the primary benefit of providing an impartial assessment of complex protein mixtures. Despite significant advancement in the genetic characterization of BrS, the identification of reliable, reproducible and specific circulating biomarkers from patients affected by this life-threatening cardiac disorder is still unsatisfactory and far to be defined.

Here, proteomics has been effectively used for identifying a subset of plasma biomarkers useful for pathogenetic and diagnostic evaluation. A total of 68 differentially expressed proteins (30 upregulated and 38 downregulated) were detected by 2D-PAGE coupled with LC-MS/MS in plasma samples from BrS patients as opposed to controls. We propose as brugada plasma biomarkers the proteins Apoliprotein E Vitronectin and α-1-antitrypsin, whose dysregulation was confirmed by Western blot analysis coherently with our previosuly work. [8]

Furthermore to enhance the power of novel biomarkers detection from the available plasma samples, proteomic analysis was integrated by the study of circulating miRNAs in the same population.

miRNA profiling offers great opportunity of investigation, aiming at understanding the molecular mechanisms underlying gene expression in cardiovascular development and disease. The role of miRNAs turns out to be determinant under different conditions, including arrhythmias. [67] Among the miRNAs whose expression is coherently substantiated from previous published data, we found of particular importance miR-92a, miR-320b and miR-425-5p The dysregulation of these miRNAs were clearly confirmed by specific taqman assay.

Overexpression of miR-92a may lead simultaneously to cardiomyopathy and arrhythmogenesis by directly repressing two distinct targets: Pten, a regulator of heart size, and Cx43, a key regulator of cardiac rhythmicity [68]. Moreover, down regulation of miR-92a decreases the inflammation process with a consequent cardioprotective effect against ischemia/reperfusion (I/R) injury. [69]

miR-320b is involved in the regulation of I/R-induced cardiac injury and dysfunction by targeting the heat-shock protein Hsp20. [70] Recently, the use of antagonist useful to alter the expression levels of miR-320b demonstrated protection against myocardial I/R injury, triggering the suppression of pro-apoptotic pathways and the activation of anti-apoptotic signals.

miR-425-5p is known to regulate blood pressure by binding a SNPs region of the NPPA gene, encoding for atrial natriuretic peptide (ANP). [71] Additionally, miR-425-p was included in a list of cardiac miRNAs, whose expression is modulated in response to physical exercise, suggesting a cardioprotective role in overstressed myocardium. [72]

Our findings support a cooperative activity of mutated genes, deregulated miRNAs and proteins in orchestrating transcriptional and post-translational events that are determinant for the development of another disease, namely the BrS, which has not been investigated thoroughly as for the other pathologic conditions discussed above. The strategies described here are complementary and represent an integrated workflow, which leads to an original, more comprehensive and high-throughput approach. In this regard, IPA tool turns up to be very helpful in combining proteomics with other high-throughput "-omics" tools and greatly contributes to a systematic understanding of the cardiovascular system.

Using IPA, it was possible to predict the activation of the ERK1/2 pathway, which was confirmed by western blot analysis and, clearly related to all BrS patients enrolled in the

study, although genetic variants which are currently found in some diagnosed patients, were not observed in the entire group (14/15 cases).

ERK1/2 activation was further confirmed in a test set, that includes all subjects, heterozygous nonsense variant (Q1118X) in the *SCN5A* gene,, enrolled for previosuly published study [8].

Additionally, IPA analysis, integrating quantitative information of "omics" data sets and western blot evidence on activation of ERK1/2 signaling pathway, allowed us to predict an overproduction of ROS, likewise reported by several groups. [73-75].

The implication of ROS signaling and toxicity has been described in many disease states and it is a major target in studies aimed at improving prevention and therapy. Several metabolic pathways are known to produce ROS, including ERK1/2 signaling activation. [76-77]

Recently, Liu and colleagues demonstrated that pyridine nucleotides regulate the cardiac Na^+ channel through the generation of ROS. It was reported that mutations in glycerol-3-phosphate dehydrogenase 1-like protein (*GPD1-L*), a gene associated with BrS, cause an increase of intracellular NADH levels, which in turn, augmented ROS production. The increase of oxidative stress directly influences the activity of sodium channel through the reduction of the sodium current that eventually results in altered metabolism and arrhythmic risk. [78]

CONCLUSION

All together, the data reported here strongly support the hypothesis that in BrS a fine balance among mutated genes, deregulated proteins, and miRNAs might exist. In our model, we predict that, under physiological conditions, the myocardium of BrS patients presents a constitutive activation of the ERK1/2 pathway and a moderate increase of ROS levels, which, in turn, modulate the sodium channel activity. Stressing conditions such as, fever or some drugs to be avoided, might produce a significant perturbation of this system, with the

consequential breakdown of the fine equilibrium and the unveiling of life-threatening tachyarrhythmias.

In conclusion, our study highligts the power of an integrated, multi-omics approach in the pathophysiology of BrS and provides a strong basis to deepen the investigation on ERK1/2-ROS cross talk and to elucidate how ERK1/2 pathway modulates cardiovascular cellular signaling under homeostatic and pathological conditions.

A further elucidation of these mechanisms will allow us to gain an in-depth understanding of the pathogenesis as well as the progression and outcome of BrS.

REFERENCES

1. Brugada J, Brugada R, Brugada P. Right bundle-branch block and ST-segment elevation in leads V1 through V3: a marker for sudden death in patients without demonstrable structural heart disease. Circulation. 1998 Feb 10;97(5):457-60.

2. Curcio A1, Santarpia G, Indolfi C. The Brugada Syndrome - From Gene to Therapy. Circ J. 2017 Feb 24;81(3):290-297. doi: 10.1253/circj.CJ-16-0971. Epub 2017 Jan 7.

3. Lindsey ML, Mayr M, Gomes AV, Delles C, Arrell DK, Murphy AM, Lange RA, Costello CE, Jin YF, Laskowitz DT, Sam F, Terzic A, Van Eyk J, Srinivas PR.. American Heart Association Council on Functional Genomics and Translational Biology, Council on Cardiovascular Disease in the Young, Council on Clinical Cardiology, Council on Cardiovascular and Stroke Nursing, Council on Hypertension, and Stroke Council. Transformative Impact of Proteomics on Cardiovascular Health and Disease: A Scientific Statement From the American Heart Association. Circulation. 2015;132(9):852-72.

4. Hanash SM, Pitteri SJ, Faca VM. Mining the plasma proteome for cancer biomarkers. Nature. 2008;452(7187):571-579.

5. Martin A. Maly, Pavel Majek, Zuzana Reicheltova, Roman Kotlin, Jiri Suttnar, Milan Oravec, Josef Veselka, Jan E. Dyr . Proteomic analysis of plasma samples from acute coronary syndrome patients — The pilot study. International Journal of Cardiology, Vol. 157, Issue 1, p126–128

6. Scumaci D, Gaspari M, Saccomanno M, Argirò G, Quaresima B, Faniello CM, Ricci P, Costanzo F, Cuda G.. Assessment of an ad hoc procedure for isolation and characterization of human albuminome. Anal Biochem 2011; 418(1):161-163.

7. Boschetti E, Righetti PG. The ProteoMiner in the proteomic arena: a non-depleting tool for discovering low-abundance species. J Proteomics. 2008; 71(3):255-264.

8. Di Domenico M, Scumaci D, Grasso S, Gaspari M, Curcio A, Oliva A, Ausania F, Di Nunzio C, Ricciardi C, Santini AC, Rizzo FA, Romano Carratelli C, Lamberti M, Conti D, La Montagna R, Tomei V, Malafoglia V, Pascali VL, Ricci P, Indolfi C, Costanzo F, Cuda G. Biomarker discovery by plasma proteomics in familial Brugada Syndrome. Front Biosci (Landmark Ed). 2013;18:564-571.

9. Mitchell PS, Parkin RK, Kroh EM, Fritz BR, Wyman SK, Pogosova-Agadjanyan EL, Peterson A, Noteboom J, O'Briant KC, Allen A, Lin DW, Urban N, Drescher CW, Knudsen BS, Stirewalt DL, Gentleman R, Vessella RL, Nelson PS, Martin DB, Tewari M. Circulating microRNAs as stable blood-based markers for cancer detection. Proc Natl AcadSci USA. 2008; 105:10513–10518.

10. Lawrie CH, Gal S, Dunlop HM, Pushkaran B, Liggins AP, Pulford K, Banham AH, Pezzella F, Boultwood J, Wainscoat JS, Hatton CS, Harris AL. Detection of elevated levels of tumour-associated microRNAs in serum of patients with diffuse large B-cell lymphoma. Br J Haematol. 2008; 141:672–675.

11. Stanczyk J, Pedrioli DM, Brentano F, Sanchez-Pernaute O, Kolling C, Gay RE, Detmar M, Gay S, Kyburz D. Altered expression of MicroRNA in synovial fibroblasts and synovial tissue in rheumatoid arthritis. Arthritis Rheum. 2008; 58:1001–1009.

12. Busch A, Eken SM, Maegdefessel. Prospective and therapeutic screening value of non-coding RNA as biomarkers in cardiovascular disease. Ann Transl Med. 2016;4(12):236.

13. Huibo Wang, Jun Yang, Jian Yang, Zhixing Fan, Chaojun Yang. Circular RNAs: Novel rising stars in cardiovascular disease research. International Journal of Cardiology, Vol. 202, p726–727. DOI: 10.1016/j.ijcard.2015.10.051

14. McKenna A, Hanna M, Banks E, Sivachenko A, Cibulskis K, Kernytsky A, , Garimella K, Altshuler D, Gabriel S, Daly M, DePristo MA. The Genome Analysis Toolkit: a MapReduce framework for analyzing next-generation DNA sequencing data. Genome research. 2010;20(9):1297-303.

15. Hallam S, Nelson H, Greger V, Perreault-Micale C, Davie J, Faulkner N, Neitzel D, Casey K, Umbarger MA, Chennagiri N, Kramer AC, Porreca GJ, Kennedy CJ. Validation for Clinical Use of, and Initial Clinical Experience with, a Novel Approach to Population-Based Carrier Screening using High-Throughput, Next-Generation DNA Sequencing. The Journal of molecular diagnostics: JMD. 2014;16(2):180-9.

16. 1000 Genomes Project Consortium, Abecasis GR, Auton A, Brooks LD, DePristo MA, Durbin RM, Handsaker RE, Kang HM, Marth GT, McVean GA.An integrated map of genetic variation from 1,092 human genomes. Nature. 2012;491(7422):56-65. 6. Stenson PD, Ball EV, Mort M, Phillips AD, Shiel JA, Thomas NS, Abeysinghe S, Krawczak M, Cooper DN. Human Gene Mutation Database (HGMD): 2003 update. Human mutation. 2003;21(6):577-81.

17. Choi Y, Sims GE, Murphy S, Miller JR, Chan AP. Predicting the functional effect of amino acid substitutions and indels. PloS one. 2012;7(10):e46688.

18. Adzhubei I, Jordan DM, Sunyaev SR. Predicting functional effect of human missense mutations using PolyPhen-2. Curr Protoc Hum Genet. 2013 Jan; Chapter 7:Unit7.20.

19. Reva B, Antipin Y, Sander C. Determinants of protein function revealed by combinatorial entropy optimization. Genome biology. 2007;8(11):R232.

20. Bradford MM. A rapid and sensitive method for the quantitation of microgram quantities of protein utilizing the principle of protein-dye binding. Anal Biochem. 1976; 72:248-254.

21. Cleveland DW, Fischer SG, Kirschner MW, Laemmli UK. Peptide mapping by limited proteolysis in sodium dodecyl sulfate and analysis by gel electrophoresis. J Biol Chem. 1977; 252(3):1102-1106.

22. Weiss W, Gorg A. High-resolution two-dimensional electrophoresis. Methods Mol. Biol. 2009; 564, 13–32.

23. Milan E, Lazzari C, Anand S, Floriani I, Torri V, Sorlini C, Gregorc V, Bachi A. SAA1 is over-expressed in plasma of non small cell lung cancer patients with poor outcome after treatment with epidermal growth factor receptor "tyrosine-kinase inhibitors. J Proteomics. 2012;76 Spec No.:91-101.

24. Dutta M, Subramani E, Taunk K, Gajbhiye A, Seal S, Pendharkar N, Dhali S, Ray CD, Lodh I, Chakravarty B, Dasgupta S, Rapole S, Chaudhury K. Investigation of serum proteome alterations in human endometriosis. J Proteomics. 2015 J;114:182-96.

25. Seillier-Moiseiwitsch F: The Proteomics Protocols Handbook. 2005; 239-258.

26. Shevchenko A, Wilm M, Vorm O, Mann M. Mass spectrometric sequencing of proteins silver-stained polyacrylamide gels. Anal Chem. 1996;68(5):850-8

27. Sinha P, Poland J, Schnolzer M, and Rabilloud T. A new silver staining apparatus and procedure for matrix-assisted laser desorption/ionization-time of flight analysis of proteins after two-dimensional electrophoresis. Proteomics. 2001; 1,835–840 27.

28. Gharahdaghi F, Weinberg C.R, Meagher D.A, Imai, B.S, Mische S.M. Mass spectrometry identification of proteins from silver stained polyacrylamide gel: a method for the removal of silver ions to enhance sensitivity. Electrophoresis. 1999; 20, 601–605.

29. Zivy M. Quantitative analysis of 2D gels. Methods Mol Biol. 2007;355:175-194.

30. Hellman U, Wernsted C, Gonez J, Heldin C.H. Improvement of an "In-Gel" digestion procedure for the micropreparation of internal protein fragments for amino acid sequencing. Anal. Biochem. 1995; 224, 451–455.

31. Rappsilber J, Ishihama Y, and Mann M. Stop and go extraction tips for matrix-assisted laser desorption/ionization, nanoelectrospray, and LC/MS sample pretreatment in proteomics. Anal Chem. 2003; 75, 663-670.

32. Krämer A, Green J, Pollard J, Tugendreich S. Causal Analysis Approaches in Ingenuity Pathway Analysis (IPA). Bioinformatics. 2014;30(4):523-30. doi: 10.1093/bioinformatics/btt703.

33. Polovina MM1, Vukicevic M2, Banko B3, Lip GYH4, Potpara TS5. Brugada syndrome: A general cardiologist's perspective Eur J Intern Med. 2017 Oct;44:19-27. doi: 10.1016/j.ejim.2017.06.019

34. Antzelevitch C, Brugada P, Borggrefe M, Brugada J, Brugada R, Corrado D, Gussak I, LeMarec H, Nademanee K, Perez Riera AR, Shimizu W, Schulze-Bahr E, Tan H, Wilde A. Brugada Syndrome: Report of the Second Consensus Conference: Endorsed by the Heart Rhythm Society and the European Heart Rhythm Association. Circulation. 2005;111:659-670.

35. Neganova I, Vilella F, Atkinson SP, Lloret M, Passos JF, von Zglinicki T, O'Connor JE, Burks D, Jones R, Armstrong L, Lako M. An important role for CDK2 in G1 to S checkpoint activation and DNA damage response in human embryonic stem cells. Stem Cells. 2011 Apr;29(4):651-9.

36. So J, Pasculescu A, Dai AY, Williton K, James A, Nguyen V, Creixell P, Schoof EM, Sinclair J, Barrios-Rodiles M, Gu J, Krizus A, Williams R, Olhovsky M, Dennis JW, Wrana JL, Linding R, Jorgensen C, Pawson T, Colwill K. Integrative analysis of kinase networks in TRAIL-induced apoptosis provides a source of potential targets for combination therapy. Sci Signal. 2015 Apr 07;8(371):rs3. Epub 2015 Apr 7.

37. Zhao R, Yang HY, Shin J, Phan L, Fang L, Che TF, Su CH, Yeung SC, Lee MH. CDK inhibitor p57 (Kip2) is downregulated by Akt during HER2-mediated tumorigenicity. Cell Cycle. 2013 Mar 15;12(6):935-43.

38. Luciani MG, Hutchins JR, Zheleva D, Hupp TR. The C-terminal regulatory domain of p53contains a functional docking site for cyclin A. J Mol Biol. 2000 Jul 14;300(3):503-18.

39. Garibaldi F1, Falcone E1, Trisciuoglio D1, Colombo T2,3, Lisek K4,5, Walerych D4, Del Sal G4,5, Paci P2,3, Bossi G1,6, Piaggio G1, Gurtner A1. Mutant p53 inhibits miRNA biogenesis by interfering with the microprocessor complex. Oncogene. 2016 Jul 21;35(29):3760-70. doi: 10.1038/onc.2016.51.

40. Tarasov V, Jung P, Verdoodt B, Lodygin D, Epanchintsev A, Menssen A, Meister G, Hermeking H. Differential regulation of microRNAs by p53 revealed by massively parallel sequencing: miR-34a is a p53 target that induces apoptosis and G1-arrest. Cell Cycle. 2007 Jul 01;6(13):1586-93. Epub 2007 May 11.

41. Ren XP, Wu J, Wang X, Sartor MA, Jones K, Qian J, Nicolaou P, Pritchard TJ, Fan GC. MicroRNA-320 is involved in the regulation of cardiac ischemia/reperfusion injury by targeting heat-shock protein 20. Circulation. 2009 May 05;119(17):2357-2366. Epub 2009 Apr 20.

42. Andrikopoulos P, Fraser SP, Patterson L, Ahmad Z, Burcu H, Ottaviani D, Diss JK, Box C, Eccles SA, Djamgoz MB. Angiogenic functions of voltage-gated Na+ Channels in human

endothelial cells: modulation of vascular endothelial growth factor (VEGF) signaling. J Biol Chem. 2011 May 13;286(19):16846-60.

43. Li Y, Song D, Song Y, Zhao L, Wolkow N, Tobias JW, Song W, Dunaief JL. Iron-induced Local Complement Component 3 (C3) Up-regulation via Non-canonical Transforming Growth Factor (TGF)-β Signaling in the Retinal Pigment Epithelium. J Biol Chem. 2015 May 08;290(19):11918-34.

44. Chen Y, Löhr M, Jesnowski R. Inhibition of ankyrin-B expression reduces growth and invasion of human pancreatic ductal adenocarcinoma. Pancreatology. 2010;10(5):586-96. Epub 2010 Oct 30.

45. Griselli M, Herbert J, Hutchinson WL, Taylor KM, Sohail M, Krausz T, Pepys MB. C-reactive protein and complement are important mediators of tissue damage in acute myocardial infarction. J Exp Med. 1999 Dec 20;190(12):1733-40.

46. Petzelbauer P, Zacharowski PA, Miyazaki Y, Friedl P, Wickenhauser G, Castellino FJ, Gröger M, Wolff K, Zacharowski K. The fibrin-derived peptide B beta15-42 protects the myocardium against ischemia-reperfusion injury. Nat Med. 2005 Mar;11(3):298-304.

47. Velu CS, Baktula AM, Grimes HL. Gfi1 regulates miR-21 and miR-196b to control myelopoiesis. Blood. 2009 May 07;113(19):4720-8.

48. Lebedeva IV, Washington I, Sarkar D, Clark JA, Fine RL, Dent P, Curiel DT, Turro NJ, Fisher PB. Strategy for reversing resistance to a single anticancer agent in human prostate and pancreatic carcinomas. Proc Natl Acad Sci U S A. 2007 Feb 27;104(9):3484-9.

49. Yang BX, Duan YJ, Dong CY, Zhang F, Gao WF, Cui XY, Lin YM, Ma XT. Novel functions for mda-7/IL-24 and IL-24 delE5: regulation of differentiation of acute myeloid leukemic cells. Mol Cancer Ther. 2011 Apr;10(4):615-25..

50. Vidal LJ, Perry JK, Vouyovitch CM, Pandey V, Brunet-Dunand SE, Mertani HC, Liu DX, Lobie PE. PAX5alpha enhances the epithelial behavior of human mammary carcinoma cells. Mol Cancer Res. 2010 Mar;8(3):444-56.

51. Maarof G, Bouchet-Delbos L, Gary-Gouy H, Durand-Gasselin I, Krzysiek R, Dalloul A. Interleukin-24 inhibits the plasma cell differentiation program in human germinal center B cells. Blood. 2010 Mar 04;115(9):1718-26.

52. Commins S, Steinke JW, Borish L. The extended IL-10 superfamily: IL-10, IL-19, IL-20, IL-22, IL-24, IL-26, IL-28, and IL-29. J Allergy Clin Immunol. 2008 May;121(5):1108-11. Epub 2008 Apr 11.

53. Dasgupta M, Dermawan JK, Willard B, Stark GR. STAT3-driven transcription depends upon the dimethylation of K49 by EZH2. Proc Natl Acad Sci U S A. 2015 Mar 31;112(13):3985-90.

54. Shen L, Tso P, Woods SC, Sakai RR, Davidson WS, Liu M. Hypothalamic apolipoprotein A-IV is regulated by leptin. Endocrinology. 2007 Jun;148(6):2681-9.

55. Hagiwara M, Kokubu E, Sugiura S, Komatsu T, Tada H, Isoda R, Tanigawa N, Kato Y, Ishida N, Kobayashi K, Nakashima M, Ishihara K, Matsushita K. Vinculin and Rab5 complex is required [correction of requited]for uptake of Staphylococcus aureus and interleukin-6 expression. PLoS One. 2014;9(1):e87373.

56. Rein-Smith CM, Anderson NW, Farrell DH. Differential regulation of fibrinogen γ chain splice isoforms by interleukin-6. Thromb Res. 2013 Jan;131(1):89-93.

57. Hattori M, Abraham LJ, Northemann W, Fey GH. Acute-phase reaction induces a specific complex between hepatic nuclear proteins and the interleukin 6 response element of the rat alpha 2-macroglobulin gene. Proc Natl Acad Sci U S A. 1990 Mar;87(6):2364-8.

58. Subauste MC, Nalbant P, Adamson ED, Hahn KM. Vinculin controls PTEN protein level by maintaining the interaction of the adherens junction protein beta-catenin with the scaffolding protein MAGI-2. J Biol Chem. 2005 Feb 18;280(7):5676-81.

59. Burger ML, Xue L, Sun Y, Kang C, Winoto A. Premalignant PTEN-deficient thymocytes activate microRNAs miR-146a and miR-146b as a cellular defense against malignant transformation. Blood. 2014 Jun 26;123(26):4089-100.

60. Hoshi M1, Du XX, Shinlapawittayatorn K, Liu H, Chai S, Wan X, Ficker E, Deschênes I. Brugada syndrome disease phenotype explained in apparently benign sodium channel mutations.Circ Cardiovasc Genet. 2014Apr;7(2):123-31.

61. Tangney JR, Chuang JS, Janssen MS, Krishnamurthy A, Liao P, Hoshijima M, Wu X, Meininger GA, Muthuchamy M, Zemljic-Harpf A, Ross RS, Frank LR, McCulloch AD, Omens JH. Novel role for vinculin in ventricular myocyte mechanics and dysfunction. Biophysical journal. 2013;104(7):1623-33.

62. Sternick EB, Oliva A, Gerken LM, Magalhães L, Scarpelli R, Correia FS, Rego S, Santana O, Brugada R, Wellens HJ. Clinical, electrocardiographic, and electrophysiologic characteristics of patients with a fasciculoventricular pathway: the role of PRKAG2 mutation. Heart Rhythm. 2011 Jan;8(1):58-64. doi: 10.1016/j.hrthm.2010.09.081. Epub 2010 Oct 1. PubMed PMID: 20888928.

63. Hashemi SM, Hund TJ, Mohler PJ. Cardiac ankyrins in health and disease. Journal of molecular and cellular cardiology. 2009;47(2):203-9.

64. Mestroni L, Taylor MR. Genetics and genetic testing of dilated cardiomyopathy: a new perspective. Discovery medicine. 2013;15(80):43-9.

65. Danielson LS, Park DS, Rotllan N, Chamorro-Jorganes A, Guijarro MV, Fernandez-Hernando C, Fishman GI, Phoon CK, Hernando E. Cardiovascular dysregulation of miR-17-

92 causes a lethal hypertrophic cardiomyopathy and arrhythmogenesis. FASEB J. 2013; 27(4),1460–1467.

66. Salloum FN1, Yin C, Kukreja RC. Role of microRNAs in cardiac preconditioning. J Cardiovasc Pharmacol. 2010;56(6):581-8.

67. Zhang Y, Cheng J, Chen F, Wu C, Zhang J, Ren X, Pan Y, Nie B, Li Q, Li Y. Circulating endothelial microparticles and miR-92a in acute myocardial infarction. Biosci Rep. 2017; 37(2).

68. Song CL, Liu B, Diao HY, Shi YF, Zhang JC, Li YX, Liu N, Yu YP, Wang G, Wang JP, Li Q. Down-regulation of microRNA-320 suppresses cardiomyocyte apoptosis and protects against myocardial ischemia and reperfusion injury by targeting IGF-1.Oncotarget. 2016;7(26):39740-39757.

69. Arora P, Wu C, Khan AM, Bloch DB, Davis-Dusenbery BN, Ghorbani A, SpagnolliE,Martinez A, Ryan A, Tainsh LT, Kim S, Rong J, Huan T, Freedman JE, Levy D, Miller KK, Hata A, Del Monte F, Vandenwijngaert S, Swinnen M, Janssens S, Holmes TM, Buys ES, Bloch KD, Newton-Cheh C, Wang TJ. Atrial natriuretic peptide is negatively regulated by microRNA-425. J Clin Invest. 2013;123(8):3378-3382. doi: 10.1172/JCI67383

70. Souza RW, Fernandez GJ, Cunha JP, Piedade WP, Soares LC, Souza PA, de Campos DH, Okoshi K, Cicogna AC, Dal-Pai-Silva M, Carvalho RF. Regulation of cardiac microRNAs induced by aerobic exercise training during heart failure. Am J Physiol Heart Circ Physiol. 2015;309(10):H1629-41.

71. Santillo M, Mondola P, Serù R, Annella T, Cassano S, Ciullo I, Tecce MF, Iacomino G, Damiano S, Cuda G, Paternò R, Martignetti V, Mele E, Feliciello A, Avvedimento EV. Opposing functions of Ki- and Ha-Ras genes in the regulation of redox signals. Curr Biol. 2001 ;11(8):614-9.

72. Ushio-Fukai M, Alexander RW. Reactive oxygen species as mediators of angiogenesis signaling: role of NAD(P)H oxidase. Mol Cell Biochem. 2004 ;264(1-2):85-97.

73. Miller RL, Sun GY, Sun AY. Cytotoxicity of paraquat in microglial cells: Involvement of PKCdelta- and ERK1/2-dependent NADPH oxidase. Brain Res. 2007 ;1167:129-39.

74. Choudhary S, Wang KK, Wang HC. Oncogenic H-Ras, FK228, and exogenous H2O2 cooperatively activated the ERK pathway in selective induction of human urinary bladder cancer J82 cell death. Mol Carcinog. 2011;50(3):215-9.

75. Apolloni S, Parisi C, Pesaresi MG, Rossi S, Carrì MT, Cozzolino M, Volonté C, D'Ambrosi N. The NADPH oxidase pathway is dysregulated by the P2X7 receptor in the SOD1-G93A microglia model of amyotrophic lateral sclerosis. J Immunol. 2013;190(10):5187-95.

76. Liu M, Liu H, Dudley SC Jr. Reactive oxygen species originating from mitochondria regulate the cardiac sodium channel. Circ Res. 2010;107(8):967-74.

77. Marco-Sola S1, Sammeth M, Guigó R, Ribeca P. The GEM mapper: fast, accurate and versatile alignment by filtration. Nat Methods. 2012 ;9(12):1185-8.

78. Li H[1], Handsaker B, Wysoker A, Fennell T, Ruan J, Homer N, Marth G, Abecasis G, Durbin R; 1000 Genome Project Data Processing Subgroup. The Sequence Alignment/Map format and SAMtools. Bioinformatics. 2009;25(16):2078-9.

TABLE LEGENDS

Table 1

ACTC1, ACTN2, ANK2, CACNA1C, CACNB2, CASQ2, CAV3, CRYAB, CSRP3, DES, DMD, DSC2, DSG2, DSP, EMD, FBN1, GLA, GPD1L, HCN4, JPH2, JUP, KCNE1, KCNE2, KCNH2, KCNJ2, KCNQ1, LAMP2, LDB3, LMNA, MYBPC3, MYH6, MYH7, MYL2, MYL3, MYOZ2, PDLIM3, PKP2, PLN, PRKAG2, RYR2, SCN4B, SCN5A, SGCA, SGCB, SGCD, TAZ, TCAP, TGFB3, TGFBR2, TNNC1, TNNI3, TNNT2, TPM1, TTN, VCL

Table 1

List of the 55 SD-related genes included in our panel.

Table 2

Genetic variations identified in each case. At least one rare variant was identified in each case analyzed except one (index case 15). In column 3, A or C means if a gene is Associated with BrS or is a Candidate gene. In column 7, data refer to dbSNP (Single Nucleotide Polymorphism database) or HGMD (Human Gene Mutation Database) databases. Column 8 show deleterious prediction of 3 databases (PROVEAN -Protein Variation Effect Analyzer-, PolyPhen-2 Polymorphism Phenotyping v2-, and Mutation Assessor). NA (Data Not Available).

Index Case	Gene_RefSeq	Candidate/ Associated	cDNA variant	Aa variant	Exome Aggregation Consortium (ExAC)	Code dbSNP/HGMD	Deleterious *In Silico* Predictors	Segregation Studies
					Segregation			
1	*SCN5A*_ NM_198056	A	c.4243G>A	p.V1415M	-	-	2/3	Yes
2	*TTN*_NM_133378	C	c.63894A>C	p.K21298N	NA	-	3/3	Yes
	*PRKAG2*_NM_016203	C	c.1568G>A	p.R523K	-	-	0/3	No
3	*SCN5A*_NM_198056	A	c.5406C>G	p.D1802E	-	-	3/3	Yes
	*TTN*_NM_133378	C	c.93578G>A	p.R31193Q	NA	-	3/3	No
	*TTN*_NM_133378	C	c.44345A>G	p.K14782R	NA	-	0/3	Yes
4	*SCN5A*_NM_006514	A	c.4501C>G	p.L1501V	3/121386	rs199473266 / CM002389	3/3	No
	*ANK2*_NM_001148	C	c.4834A>G	p.T1612A	-	-	0/3	Yes

Received: 03 23, 2018; Revised: 05 26, 2018; Accepted: 06 21, 2018

This article has been accepted for publication and undergone full peer review but has not been through the copyediting, typesetting, pagination and proofreading process, which may lead to differences between this version and the Version of Record. Please cite this article as doi: 10.1002/prca.201800065 .

Index Case	Gene_RefSeq	Candidate/ Associated	cDNA variant	Aa variant	Exome Aggregation Consortium (ExAC)	Code dbSNP/HGMD	Deleterious *In Silico* Predictors	Segregation Studies
	*VCL*_NM_014000	C	c.3051G>C	p.Q1017H	2/121254	-	1/3	Yes
5	*SCN5A*_ NM_198056	A	c.3181G>T	p.E1061X	-	-	-	Yes
				No relatives available				
6	*TTN*_NM_133378	C	c.50693C>G	p.G16898A	NA	rs201922910	3/3	NA
	*SGCA*_NM_000023	C	c.155T>G	p.V52G	5/121270	rs148132791		
7	*CACNA1D*_NM_000720	C	c.372A>C	p.E124D	2/120644	rs368995943	0/3	NA
8	*TTN*_NM_133378	C	c.75377G>A	p.R25126H	NA	-	3/3	NA
	*TTN*_NM_133378	C	c.60116C>T	p.T20039I	NA	-	2/3	
	*JUP*_NM_002230	C	c.1359G>T	p.E453D	-	rs376608339	3/3	
9	*TTN*_NM_133378	C	c.9512A>G	p.N3171S	NA	rs139992576	3/3	NA
10	*SCN5A*_ NM_198056	A	c.4498C>G	p.L1501V	3/121386	rs199473266 / CM002389	3/3	NA
	*DSC2*_ NM_024422	C	c.2194T>G	p.L732V	146/121334	rs151024019	0/3	
	*JPH2*_ NM_020433	C	c.380-6C>T	-	-	rs201197277	-	
11	*TTN*_NM_133378	C	c.90796G>A	p.E30266K	NA	rs199761901	3/3	NA
12	*DSP*_NM_004415	C	c.1736C>T	p.T579M	1/121236	-	1/3	NA
	*TTN*_NM_133378	C	c.13495C>T	p.R4499W	NA	rs377193479	3/3	

Index Case	Gene_RefSeq	Candidate/ Associated	cDNA variant	Aa variant	Exome Aggregation Consortium (ExAC)	Code dbSNP/HGMD	Deleterious *In Silico* Predictors	Segregation Studies
	*TCAP*_NM_003673	C	c.37_39delGAG	-	-	CD062239	-	
13	*TTN*_NM_133378	C	c.44345A>G	p.K14782R	NA	-	0/3	NA
				No segregation				
14	*CACNA1H*_NM_021098	C	c.1181G>A	p.R1194Q	2/13298	-	0/3	No
	*KCNA5*_NM_002234	C	c.919C>T	p.P307S	230/118352	rs17215409 / CM067995	0/3	No
15	No variants detected	-	-	-	-	-	-	-

FIGURE LEGENDS

Figure 1

Families showing complete segregation of the detected variants

A-Index case 1: a private genetic variant (p.V1415M) was detected in the *SCN5A* gene. The same variant was also identified in II:2 and II:3, both clinically affected.

B-Index case 2: two new genetic variants were identified in the *TTN* and *PRKAG2* genes. The *TTN* gene was also identified in II:2 and II:3, both relatives clinically affected. Nevertheless, the *PRKAG2* variant was only identified in II.2.

C-Index case 3: three private genetic variants were identified in the index case. Only the p.K14782R_*TTN* and p.D1802E_*SCN5A* variants were identified in II.1, clinically affected too.

D-Index case 4: three variants were identified (p. L1501V_*SCN5A*, p.T1612A_*ANK2* and p.Q1017H_*VCL*). Two private genetic variants (p.T1612A_*ANK2* and p.Q1017H_*VCL)* were also identified in II.2, clinically affected.

E: Index case 5: a new nonsense *SCN5A* variation was detected in the index case. This variant showed complete segregation because both affected I:1 and II:2 carried it.

Received: 03 23, 2018; Revised: 05 26, 2018; Accepted: 06 21, 2018

This article has been accepted for publication and undergone full peer review but has not been through the copyediting, typesetting, pagination and proofreading process, which may lead to differences between this version and the Version of Record. Please cite this article as doi: 10.1002/prca.201800065 .

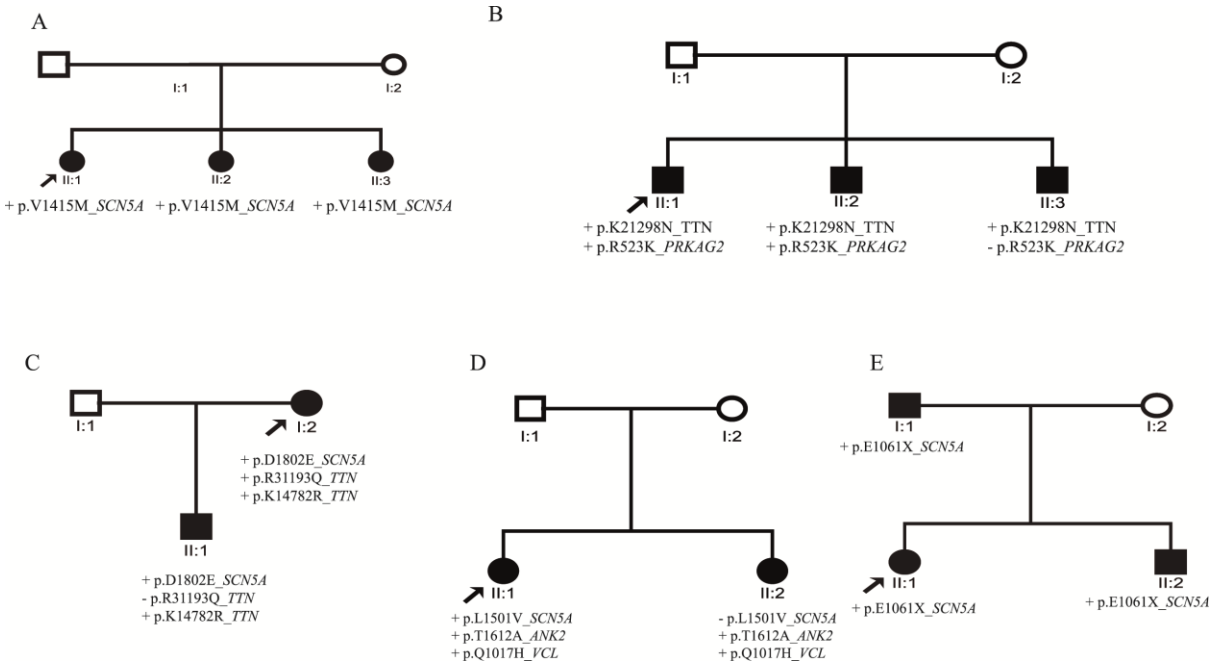

Figure 2

Panel A: Representative 2D Gel maps

Representative 2D Gel maps from a control subject (A) BrS patient positive for *SCN5A* variant (B) and BrS patients negative for *SCN5A* variant (C). Plasma samples were processed with Proteominer and separated by 2D gel electrophoresis. Isoelectrofocusing was carried out on 3-10NL IPGstrip, 24cm length. Second dimension was performed on 12% SDS-PAGE. Gel images were analyzed using Image master 2D platinum. Differentially expressed spots were digested and analyzed by LC-MS/MS.

Panel B: Western blot analysis.

Analysis was performed on crude plasma samples. 50μg of proteins were analyzed for each sample. In the figure are shown western blot for Vitronectin, Apolipoprotein E, and α1-antitrypsin. Left panels: representative western blot, Lane1-6 Brugada syndrome patients (positive for SCN5A variants: lanes 1,2,4,6; negative for SCN5A variants: lanes 3,5) ; lane 7-9 control subjects. Right panels: densitometric analysis for each blotted protein. Analysis was performed using three independent experiments. Data are mean±SEM. p value<0.05.

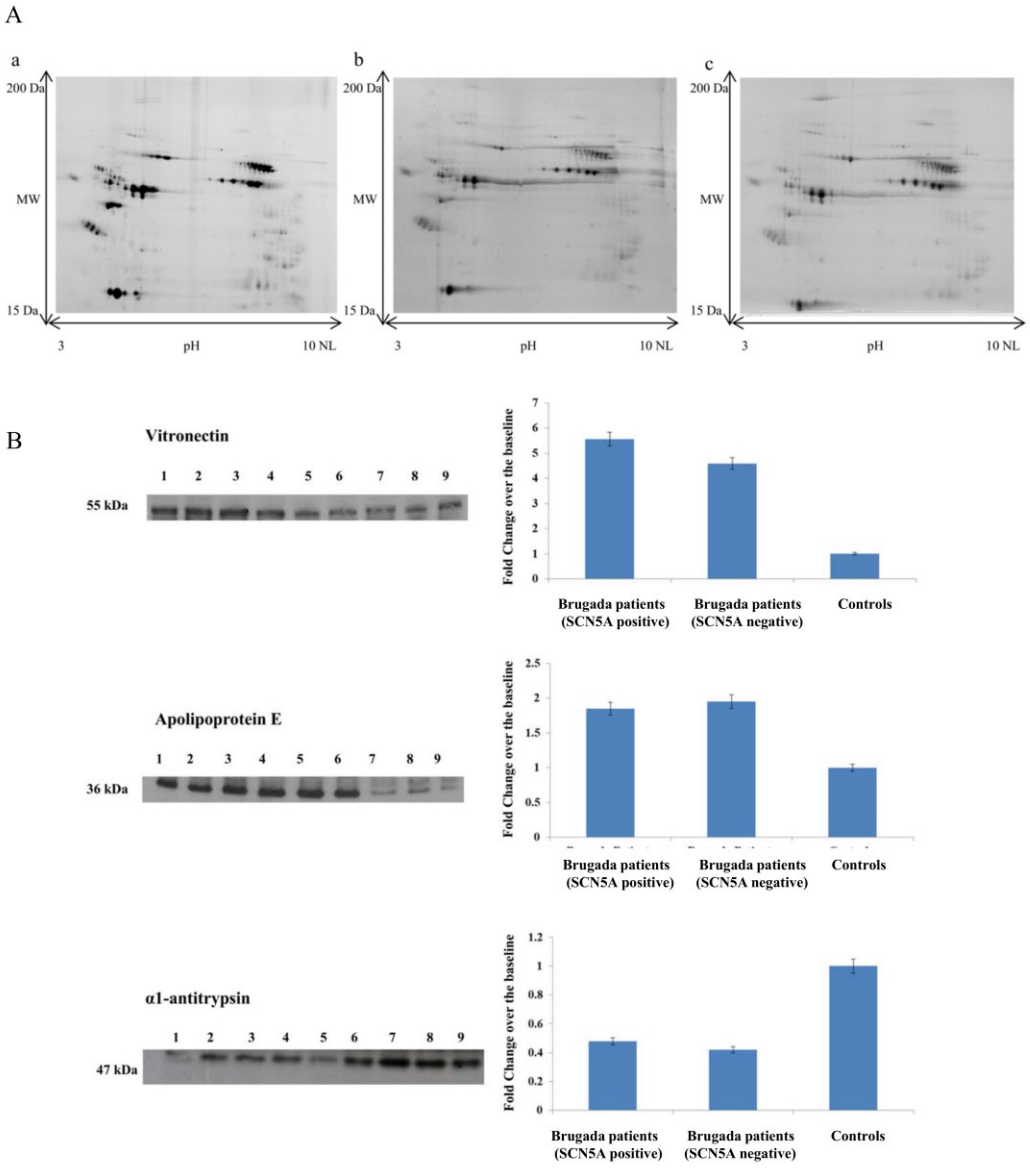

Figure 3

MiRNA profiling using Exiqon microRNA array and validation assay by Taqman qPCR.

Panel a; Bar chart showing results of the Exiqon microRNA Array. The graph shows the most significant deregulated miRNA in BrS patients positive for SCN5A variants vs healthy controls and in BrS patients negative for SCN5A variants vs controls . Analysis was performed using three independent experiments. Data was processed using genex software.

Panel b; Validation of miRNA array through Taqman assay. rtPCR was done on miR-425-5p.

Panel c; Validation of miRNA array through taqman assay. rtPCR was done on miR 92a-3p.

Panel d; Validation of miRNA array through taqman assay. rtPCR was done on miR 320b.

Analyses were performed using three independent experiments. Data are mean±SEM. p value<0.05

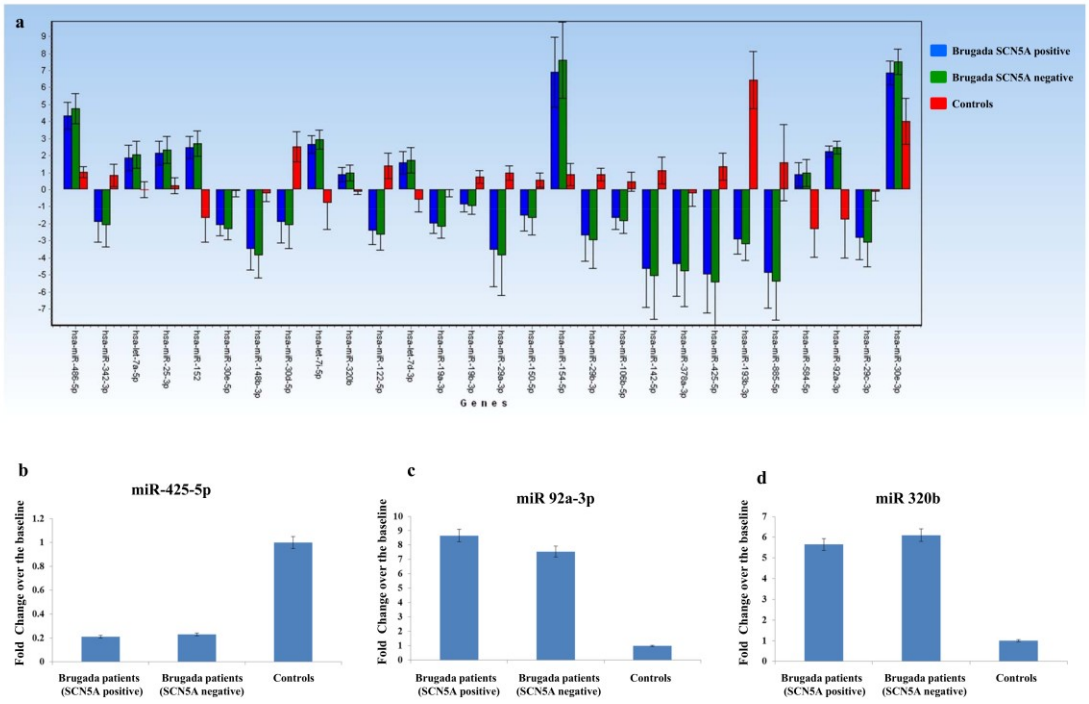

Figure 4

IPA analysis.

In the figure are shown the list of network generated using ingenuity pathway analysis software (a) and the top two Networks, namely network1 (b), network 2 (c).

d) Quantification of ERK1/2 activation from the western blots. pERK1/2 band intensity was normalized to ERK1/2 total band intensity and calculated as a ratio between BrS patients positive for SCN5A variants vs controls and in BrS patients negative for SCN5A variants vs controls Analysis was achieved using three independent experiments. Data are mean±SEM . p value<0.05

e) d) Quantification of ERK1/2 activation from the western blots in a test set. pERK1/2 band intensity was normalized to ERK1/2 total band intensity and calculated as a ratio between Brugada patients (positive for heterozygous nonsense variant (Q1118X) in the *SCN5A* gene) and healthy subjects. Analysis was done on three independent experiments. Data are mean±SEM. p value<0.05

a

ID	Molecules in Network	Score	Focus Molecules	Top Diseases and Functions
1	A2M,Akt,APOE,APOH,ATP1A2,BDNF,C3,C4A/C4B,CFH,CLU,ERK1/2,F2,FAF1,GLIPR2,HABP2,IDE,LDL,let-7a-5p (and other miRNAs w/seed GAGGUAG),MAP2K1/2,mir-205,miR-122-5p (miRNAs w/seed GGAGUGU),miR-17-5p (and other miRNAs w/seed AAAGUGC),miR-92a-3p (and other miRNAs w/seed AUUGCAC),MTUS1,NFkB (complex),NUMBL,PDLIM1,PLCD1,PRDX2,PTPN12,RAMP3,SERPINA1,SERPINC1,VIM,VTN	28	15	Cellular Movement, Cancer, Organismal Injury and Abnormalities
2	ALB,AMBP,C3,CD44,CP,ETS1,FGA,FGB,FGG,GC,HAMP,IGHG1,IL6,mir-148,miR-148a-3p (and other miRNAs w/seed CAGUGCA),OSMR,PLAU,PRKAA1,PRSS3,PTX3,ROCK1,SHOC2,SLC11A1,SLC40A1,SMARCA4,SPARC,SREBF1,TEC,TF,TGFB1,TGFB1I1,TLR3,TTN,TTR,TWIST2	28	15	Cellular Movement, Cell-To-Cell Signaling and Interaction, Organismal Injury and Abnormalities
3	AGO2,BCL6,CCND1,CD79B,DCP2,DNAJB6,ETS1,FAM3C,IGHM,ITGB4,let-7a-5p (and other miRNAs w/seed GAGGUAG),mir-221,miR-150-5p (and other miRNAs w/seed CUCCCAA),miR-17-5p (and other miRNAs w/seed AAAGUGC),miR-193a-3p (and other miRNAs w/seed ACUGGCC),miR-19b-3p (and other miRNAs w/seed GUGCAAA),miR-29b-3p (and other miRNAs w/seed AGCACCA),miR-30c-5p (and other miRNAs w/seed GUAAACA),miR-320b (and other miRNAs w/seed AAAGCUG),miR-378a-3p (and other miRNAs w/seed CUGGACU),miR-486-5p (and other miRNAs w/seed CCUGUAC),miR-584-5p (and other miRNAs w/seed UAUGGUU),miR-92a-3p (and other miRNAs w/seed AUUGCAC),MMP3,MYBL2,NCOR2,PAX5,PPM1D,PRSS2,PTTG1,Rb,RFFL,TP53,WDR5,ZFP36L1	26	14	Cancer, Organismal Injury and Abnormalities, Reproductive System Disease
4	ACTB,APOA4,AXL,CASP14,CDH1,CDH2,CTGF,EIF4EBP1,ERBB2,GPI,HP1BP3,IGF1R,LDL,let-7d-3p (miRNAs w/seed UAUACGA),LIMA1,MCAM,MET,miR-30a-3p (and other miRNAs w/seed UUUCAGU),miR-342-3p (miRNAs w/seed CUCACAC),MMP1,NRG1,p85 (pik3r),PLAUR,PTEN,RAC1,Ras,RHOA,RNA polymerase I,RNA28S5,Rock,RPS15,SNAI2,SPHK1,STAU1,WISP2	9	6	Cellular Movement, Cancer, Organismal Injury and Abnormalities
5	FCAR,IGHA1	2	1	Cell-To-Cell Signaling and Interaction, Cellular Compromise, Cellular Function and Maintenance
6	FCGR1A,HRG	2	1	Hematological Disease, Hereditary Disorder, Organismal Injury and Abnormalities

b

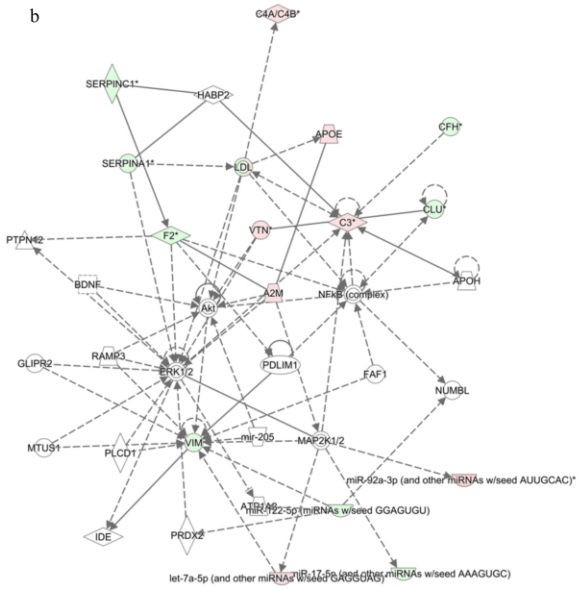

c

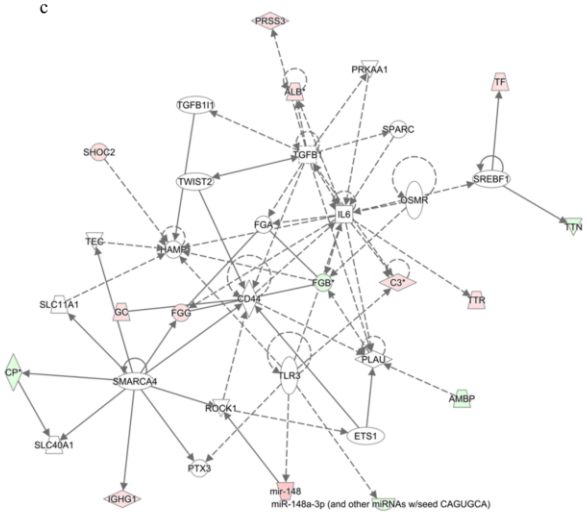

d

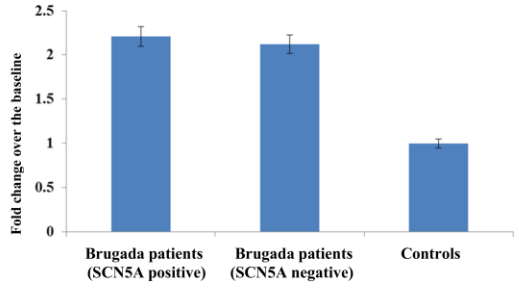

e

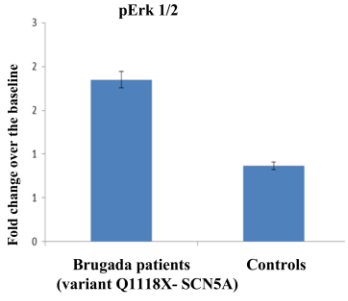

SUPPLEMENTARY TABLE LEGENDS

Supplementary Table 1

List of deregulated proteins with relative identifications. In the table, for each protein, are reported: the identification score, the number of unique peptides, the molecular mass (Da) and quantitative data. Analysis was done using three independent experiments. Data are mean±SEM . *(* p value<0.05)*

Supplementary Table 2

IPA Analysis. Cardiovascular diseases associated with deregulated proteins and miRNAs. Categories are listed based on numerosity of molecular patterns related to the disease.

SUPPLEMENTARY FIGURE LEGENDS

Supplementary Figure 1

Family showing no segregation of the detected variants. A new genetic variant in the *CACNA1H* and a previously described variant in *KCNA5* were detected in the index case. Both variants did not show segregation.

Supplementary Figure 2

1D SDS PAGE. Lane 1: Molecular Weight Markers; lane 2: crude plasma samples (control subject); lane 3: plasma samples after Proteominer enrichment (control subject), lane 4: crude plasma samples (Brugada syndrome patient); lane 5: plasma samples after Proteominer enrichment (Brugada syndrome patient). After proteominer treatment (lane 3 and 5), there is a clear decrement of high abundant protein bandS and the appearance of new bands consistent with low abundant proteins enrichment.

Supplementary Figure 3

IPA analysis. Canonical pathways classification.

Supplementary Figure 4

IPA analysis. The super network was created by merging three overlapping network. Using the MAP function (molecule activity predictor), it has been possible to predict the activation of Erk1/2 signaling

Supplementary Figure 5

IPA analysis. Mutated genes were connected with Erk 1/2 using the path explorer function. Molecules mapped in the pathways were overlapped with the dataset of deregulated proteins and mirna. Using the MAP-function, it was possible to predict the activation of Erk1/2 signaling.

Supplementary Figure 6

Network of pathways connecting the members of the omics data set with ROS generation. Using quantitative data and the IPA MAP-function, it was possible to predict ROS overexpression.

SOURCES OF FUNDING

Sources of funding

This work was supported in part by the MIUR grant PON03PE_00009_2(iCARE) to GC.

This work was supported by Obra Social "La Caixa", Fondo Investigacion Sanitaria -FIS PI14/01773 and PI17/01690- from the Instituto de Salud Carlos III (ISCIII).

AC were supported by fellowships from the PhD Programme in Molecular and translational oncology and innovative medical surgical technologies.

CVF were supported by fellowships from the PhD Programme in Molecular and translational oncology and innovative medical surgical technologies.

The CIBERCV is an initiative of the ISCIII, Spanish Ministry of Economy and Competitiveness (Fondos FEDER).

Conflicts of Interest:

The authors declare no conflict of interest." The founding sponsors had no role in the design of the study; in the collection, analyses, or interpretation of data; in the writing of the manuscript, and in the decision to publish the results.